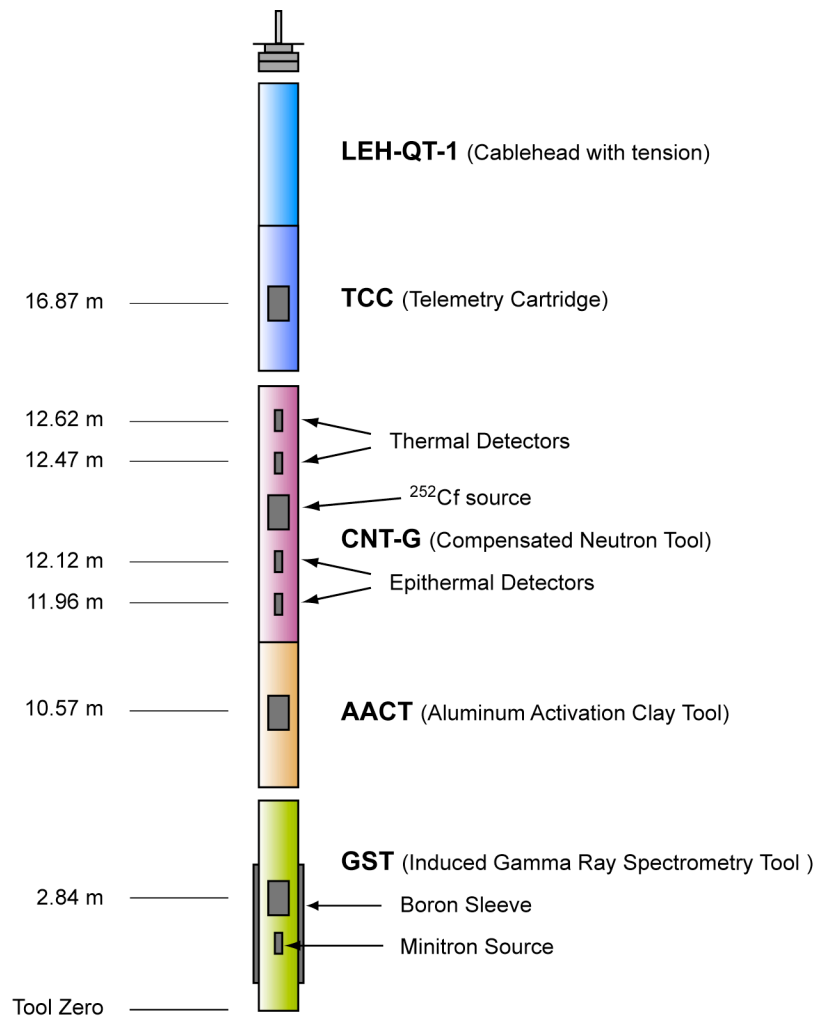


Leg 138: Geochemical Processing Report

(based on: Billeaud, L. et al. (1995). Data Report: Geochemical logging results from three lithospheric plates: Cocos, Nazca, and Pacific, Leg 138, Site 844 through 852. In Mayer, L., Pisias, N., Janecek, T. et al., Proc. ODP, Sci. Results, 138: College Station, TX (Ocean Drilling Program), 857-884.)

Geochemical Tool String

The Schlumberger geochemical tool string consists of four logging tools: the natural gamma-ray tool (NGT) the compensated neutron tool (CNT), the aluminum activation clay tool (AACT), and the gamma-ray spectrometry tool (see figure below). The natural gamma-ray tool is located at the top of the tool string, so that it can measure the naturally occurring radio nuclides, Th, U, and K, before the formation is irradiated by the nuclear sources contained in the other tools below. The compensated neutron tool, located below the natural gamma-ray tool, carries a low-energy californium source (^{252}Cf) to activate the Al atoms in the formation. The aluminum activation clay tool below subtracts the aluminum activation background radiation and a reading of formation Al is obtained (Scott and Smith, 1973).



The gamma-ray spectrometry tool, at the base of the string, carries a pulsed neutron generator to bombard the borehole and formation and an NaI(Tl) scintillation detector, which measures the spectrum of gamma rays generated by neutron-capture reactions. Because each of the elements measured (silicon, iron, calcium, titanium, sulfur, gadolinium, and potassium) is characterized by a unique spectral signature, it is possible to derive the contribution (or yield) of each of them to the measured spectrum and, in turn, to estimate their abundance in the formation. The GST also measures the hydrogen and chlorine in the borehole and formation, but the signal for these elements is almost entirely due to seawater in the borehole, and they are hence of little value.

The only major rock-forming elements not measured by the geochemical tool string are magnesium and sodium; the neutron-capture cross-sections of these elements are too small relative to their typical abundance for the tool string to detect them. A rough estimate of Mg+Na can be made by using the photoelectric factor (PEF) measured by the lithodensity tool. This measured PEF is compared with a calculated PEF (a summation of the PEF from all of the measured elements). The separation between the measured and calculated PEF is, in theory, attributable to any element left over in the formation (i.e., Mg and Na). Further explanation of this technique is found in Hertzog et al. (1989). This Mg+Na calculation was not performed for Leg 138 because including it in the normalization with the other elements induces noise into all other elements (Pratson et al., 1993).

Data Reduction

The well log data from the Schlumberger tools have been transmitted digitally up a wireline and recorded on the JOIDES Resolution in the Schlumberger Cyber Service Unit (CSU). The results from the CSU have been processed to correct for the effects of drilling fluids, logging speed, and pipe interference. Processing of the spectrometry data is required to transform the relative elemental yields into oxide weight fractions. The processing is performed with a set of log interpretation programs written by Schlumberger that have been modified to account for the lithologies and hole conditions encountered in ODP holes. The processing steps are summarized below:

Step 1: Reconstruction of relative elemental yields from recorded spectral data

The first processing step uses a weighted least-squares method to compare the measured spectra from the geochemical spectrometry tool with a series of standard spectra in order to determine the relative contribution (or yield) of each element. Whereas six elemental standards (Si, Fe, Ca, S, Cl, and H) are used to produce the shipboard yields, three additional standards (Ti, Gd, and K) can be included in the shore-based processing to improve the fit of the spectral standards to the measured spectra (Grau and Schweitzer, 1989). Although these additional elements often appear in the formation in very low concentrations, they can make a large contribution to the measured spectra, because they have large neutron-capture cross-sections. For example, the capture cross-section of Gd is 49,000 barns, that of Si 0.16 barns (Hertzog et al., 1989). Gd is therefore included in the calculation of a best fit between the measured and the standard spectra.

The spectral analysis in Leg 138 was performed using the spectral standards for H, Si, Ca, Cl, Fe, Ti, and Gd for Holes 845B, 846B, 847B, 848B, 849B, 850B, 851B, and 852D. The spectral standard for S and K were not used, because these elements exist in concentrations below the resolution of the tool, and the inclusion of S and K were found to significantly increase the noise level of all the other yields. In Hole 844B, spectral analysis using the standards H, Si, Ca, Fe, and Gd was performed. The elements S, K and Ti were not used because the concentrations of these elements are below the resolution of the tool and add noise to all other yields. A straight, seven-point (3.5 ft, 1.066 m) smoothing filter was applied to all the yields to reduce the noise in the data during this reconstruction step. An additional 10 point (5 ft, 1.523 m) smoothing filter was applied to Hole 846B, and an additional 5 point (2.5 ft, 1.313 m) smoothing filter was applied to Holes 847B, 849B, 850B, and 851B to further reduce the noise level in the normalization factor (explained in step 5), which affects the overall character of the final elemental yields.

The recomputed yields are loaded in the files

844B-yields.dat
845A-yields.dat
846B-yields.dat
847B-yields.dat
848B-yields.dat
849B-yields.dat
850B-yields.dat
851B-yields.dat.

Step 2: Depth-shifting

Geochemical processing involves the integration of data from the different tool strings; consequently, it is important that all the data are depth-correlated to one reference logging run. A total gamma-ray curve (from the gamma ray tool, which is run on each tool string) is usually chosen as a reference curve, based on cable tension (the logging run with the least amount of cable sticking) and cable speed (tools run at faster speeds are less likely to stick).

The reference run chosen for Holes 844B, 847B, 849B, 850B, and 851B is the FMS tool string. According to core-based GRAPE data, Holes 849B and 850B were then shifted up 1.83 m and 0.91 m, respectively. The GLT was the chosen reference run for Hole 845B; therefore, no depth matching was necessary. The main pass of the DIT/LSS/HLDT/NGT string was chosen as the reference run in Hole 846B. No depth matching was performed in Holes 848B and 852D because the GLT was the only log run in these holes. Hole 852D, however, was shifted 2.1 m upward to match an identified calcium carbonate peak seen on core studies (Shipboard Scientific Party, 1992).

Step 3: Calculation of total radioactivity and Th, U, and K concentrations

The third processing routine calculates the total natural gamma radiation in the formation as well as concentrations of Th, U, and K, using the counts in five spectral windows from the natural gamma-ray tool (Lock and Hoyer, 1971). This resembles shipboard processing, except that corrections for hole-size changes are made in the shore-based processing of these curves. A

Kalman filter (Ruckebusch, 1983) is applied to minimize the statistical uncertainties in the logs, which would otherwise create erroneous negative readings and anti-correlation (especially between Th and U). At each depth level calculations and corrections also were performed for K contained in the mud. This K correction is particularly useful where KCl is routinely added to the hole: because of dispersion, however, it is difficult to know exactly how much K is in the borehole. The outputs of this program are: K (wet wt %), U (ppm), and Th (ppm), along with a total gamma-ray curve and a computed gamma-ray curve (total gamma ray minus U contribution).

The processed gamma ray data are loaded in the files

844B-ngt.dat
 845A-ngt.dat
 846B-ngt.dat
 847B-ngt.dat
 848B-ngt.dat
 849B-ngt.dat
 850B-ngt.dat
 851B-ngt.dat.

Step 4: Calculation of Al concentration

The fourth processing routine calculates an Al curve using four energy windows, while concurrently correct for natural activity, borehole fluid neutron-capture cross-section, formation neutron-capture cross-section, formation slowing-down length, and borehole size. Porosity and density logs are needed in this routine to convert the wet weight percent K and Al curves to dry weight percent.

A porosity log is recorded on the geochemical tool string; however, it can only be used as a qualitative measurement, since it carries a ²⁵²Cf source, rather than the calibrated americium-beryllium source needed to make a quantitative measurement. When the density log compares well with shipboard density core measurements, a porosity curve is derived from the density log using the equation:

$$\rho_f = (\rho_m - \rho_b) / (\rho_m - \rho_f).$$

where:

ρ_f = percentage of porosity,

ρ_m = matrix density

(a constant value or log matrix density can be used in g/cm³),

ρ_b = bulk density from the log in g/cm³, and

ρ_f = density of fluid = 1.05 g/cm³.

An alternative method of calculating porosity from the log data in high porosity ranges is the neutron-derived method which uses the corrected far thermal counts (CFTC) measured with the compensated neutron tool (CNT) run with the GLT string using the ²⁵²Cf source. The CNT detects far and near thermal neutrons by counting a combination of the slowing down length and the diffusion length of the neutrons. Far and near designations are determined by the distance of

the detectors from the ^{252}Cf source. The thermal neutron detectors are highly efficient which results in good statistical behavior, as well as, being sensitive to the rock matrix composition. The far detectors have lower counting rates which leads to larger statistical uncertainties; however, the far thermal counts exhibit better porosity sensitivity than the near thermal counts. A porosity calibration of the neutron log was obtained by using the core data from Hole 846 of this leg (Truax, J., 1992). Many models were investigated by Truax; however, for the purposes of calculating porosity for reprocessing of the geochemical data, the far thermal counts were used which resulted in only 3% statistical uncertainty. After the CFTC data is smoothed by a graduated nine level filter, the equation below was applied.

$$\rho_t = 76248 \rho(CFTC'^{-1.6052}) + 36.87$$

where:

$$CFTC' = CFTC * GAIN,$$

$$(1/GAIN) = e^{(-t/1391)},$$

$$\rho_t = \text{percentage of porosity},$$

$$CFTC' = \text{calculated corrected far thermal counts},$$

$$CFTC = \text{measured corrected far thermal counts},$$

$$GAIN = \text{time function of source, and}$$

$$t = \text{time in days from calibration data;}$$

$$\text{the GLT logging date of Hole 846B (5/23/91).}$$

Both porosity calculation methods were used when the data is available. The chosen porosity curve is the one which best compares to the core porosity measurements. The porosity curve used for Holes 844B, 849B, and 851B was calculated using the density method which used the bulk density from the log and the matrix density from interpolated core data. In Hole 845B, an interpolated core porosity curve was used because the comparison of the calculated porosity to core porosity was poor. The porosity curve using the CFTC calculation compared better to core data for Holes 846B, 847B, 850B, and 852D; therefore, the neutron-derived method of calculating porosity was used. In Hole 848B, the porosity curve was derived by interpolating the core data because only the geochemical log was run and CFTC data were not recorded. Generally, in this Leg, the porosity calculated from the neutron-derived method compared better to the core measured porosity than the density porosity calculation method. Therefore, all holes where the CNT data were recorded, the neutron-derived method of porosity was used in the reprocessing of the GLT.

A correction is also made for Si interference with Al; the ^{252}Cf source activates the Si, producing the aluminum isotope, ^{28}Al (Hertzog et al., 1989). The program uses the Si yield from the gamma-ray spectrometry tool to determine the Si background correction. The program outputs dry weight percentages of Al and K, which are used in the calculation and normalization of the remaining elements.

Step 5: Normalization of elemental yields from the GST to calculate the elemental weight fractions

This routine combines the dry weight percentages of Al and K with the reconstructed yields to obtain dry weight percentages of the GST elements using the relationship:

$$W_i = F Y_i/S_i$$

where

- W_i = dry weight percentage of the i-th element
- F = normalization factor determined at each depth interval
- Y_i = relative elemental yield for the i-th element
- S_i = relative weight percentage (spectral) sensitivity of the i-th element

The normalization factor, F , is a calibration factor determined at each depth from a closure argument to account for the number of neutrons captured by a specific concentration of rock elements. Because the sum of oxides in a rock is 100%, F is given by

$$F (\sum X_i Y_i / S_i) + X_K W_K + X_{Al} W_{Al} = 100$$

where

- X_i = factor for the element to oxide (or carbonate) conversion
- X_K = factor for the conversion of K to K_2O (1.205)
- X_{Al} = factor for the conversion of Al to Al_2O_3 (1.889)
- W_K = dry weight percentage of K determined from natural activity
- W_{Al} = dry weight percentage of Al determined from the activation measurement

The sensitivity factor, S_i , is a tool constant measured in the laboratory, which depends on the capture cross-section, gamma-ray production, and detection probabilities of each element measured by the GST (Hertzog et al., 1989).

The factors X_i are simply element to oxide (or carbonate, sulfate) conversion coefficients and effectively include the O, C or S bound with each element. In processing the GLT data the correct choice of X_i is important in the closure algorithm described above and requires geological input. In most lithologies the elements measured by the tool occur in silicates where the compositions can be expressed completely as oxides.

With carbonate or carbonate-rich lithologies the measured calcium is more likely to be present as $CaCO_3$ (X_{Ca} : 2.497) than as the oxide (CaO ; X_{Ca} : 1.399). A good indication of the choice of calcium conversion factors can often be gained from shipboard X-ray diffraction (XRD) and $CaCO_3$ measurements, which estimate acid-liberated $CaCO_3$. In the absence of suitable shipboard data a rough rule of thumb is generally used such that if elemental Ca is below 6% then all Ca is assumed to be in silicate, above 12%, in carbonate. Ca concentrations between these figures are converted using linear interpolation..

The Mg and Na content curves cannot be calculated from the logs, because the neutron-capture cross sections of these elements are too small relative to their typical abundance for detection by the tool string; therefore, available core information is included. Mg + Na represent up to 8.47% of the rock in Hole 844B (Shipboard Scientific Party, 1992a). A constant value of 3.94% MgO + Na₂O was used in the normalization of Hole 844B, which was derived from the average measured core values. All other holes including Holes 845B, 846B, 847B, 848B, 849B, 850B, 851B, and 852D had insufficient or insignificant data to use in this normalization process; therefore, this process was not performed.

Steps 6-7: Calculation of oxide percentages and statistical uncertainty

These routines convert the elemental weight percentages into oxide percentages by multiplying each by its associated oxide factor (Table 1); finally the statistical uncertainty of each element is calculated, using methods described by Grau et al. (1990) and Schweitzer et al. (1988). This error is strongly related to the normalization factor, F, which is calculated at each depth level. A lower normalization factor represents better counting statistics and therefore higher quality data.

The oxide weight percentages are loaded in the files

844B-oxides.dat
845B-oxides.dat
846B-oxides.da.
847B-oxides.dat
849B-oxides.dat
850B-oxides.dat
851B-oxides.dat
851B-oxides.dat
852D-oxides.dat.

The statistical uncertainties are loaded in the files

844B-oxierr.dat
845B-oxierr.dat
846B-oxierr.dat
847B-oxierr.dat
849B-oxierr.dat
850B-oxierr.dat
851B-oxierr.dat
852D-oxierr.dat.
844B-elerr.dat
845B-elerr.dat
846B-elerr.dat
847B-elerr.dat
849B-elerr.dat
850B-elerr.dat
851B-elerr.dat
852D-elerr.dat.

Core data are loaded in the files

844B-core.dat

845B-core.dat
 846B-core.dat
 847B-core.dat
 849B-core.dat
 850B-core.dat
 851B-core.dat
 852D-core.dat.

Table 1. Oxide/carbonate factors used in normalizing elements to 100% and converting elements to oxides/carbonates.

Element	Oxide/carbonate	Conversion factor
Si	SiO ₂	2.139
Ca < 6%	CaO	1.339
6%>Ca<12%	CaO-CaCO ₃	1.399-2.497
Ca > 12%	CaCO ₃	2.497
Fe	FeO*	1.358
K	K ₂ O	1.205
Ti	TiO ₂	1.668
Al	Al ₂ O ₃	1.889

References

Grau, J. and Schweitzer, J.S. (1989). Elemental concentrations from thermal neutron capture gamma-ray spectra in geological formations. *Nuclear Geophysics* 3(1): 1-9.

Grau, J. A., Schweitzer J.S. and Hertzog, R.C. (1990). Statistical uncertainties of elemental concentrations extracted from neutron-induced gamma-ray measurements. *IEEE Transactions on Nuclear Science* 37(6): 2175-2178.

Hertzog, R., Colson, L., Seeman, B., O'Brien M., Scott, H., McKeon, D., Grau, J., Ellis, D., Schweitzer, J. and Herron, M. (1989). Geochemical logging with spectrometry tools. *SPE Formation Evaluation*, 4(2), 153-162.

Lock, G. A. and Hoyer, W. A. (1971). Natural gamma-ray spectral logging. *The Log Analyst*, 12(5): 3-9.

Pratson, E. L., Broglia, C. and Jarrard, R. (1993). Data Report: Geochemical well logs through Cenozoic and Quaternary sediments from Sites 815, 817, 820, 822, and 823. In McKenzie, J. A., Davies, P. J., Palmer-Julson, A. et al., *Proc. ODP, Sci. Results*, 133: College Station, TX (Ocean Drilling Program), 795-818.

Ruckebusch, G. (1983). A Kalman filtering approach to natural gamma ray spectroscopy in well logging. *IEEE Trans. Autom. Control*, AC-28: 372-380.

Schweitzer, J. S., Grau, J.A. and Hertzog, R.C. (1988). Precision and accuracy of short-lived activation measurements for in situ geological analyses. *Journal of Trace and Microprobe Techniques* 6(4): 437-451.

Scott, H. D. and Smith, M. P. (1973). The aluminum activation log. *The Log Analyst*, 14(5): 3-12.

Shipboard Scientific Party, 1992. *In* Mayer, L., Piasias, N., Janecek, T. et al., Proc. ODP, Init. Reports, College Station, TX (Ocean Drilling Program).

Truax, J., 1992. Wireline Neutron Log Response in High Porosity Sediments Encountered on the Ocean Drilling Project. Schlumberger-Doll Research, Ridgefield, CT.

For further information or questions about the processing, please contact:

Cristina Broglia
Phone: 845-365-8343
Fax: 845-365-3182
E-mail: chris@ldeo.columbia.edu

Trevor Williams
Phone: 845-365-8626
Fax: 845-365-3182
E-mail: trevor@ldeo.columbia.edu